An Alternative Route Based on Acid−Base Hydrolytic Chemistry to NLO Active Organic−Inorganic Hybrid Materials for Second-Order Nonlinear Optics

Hongwei Jiang and Ashok K. Kakkar*

Contribution from the Department of Chemistry, McGill University, 801 Sherbrooke Street West, Montreal, Quebec, Canada H3A 2K6

Received September 14, 1998

Abstract: An alternative approach, based on simple acid−base hydrolytic chemistry, to prepare organic−inorganic composites is reported. In these hybrid materials, NLO-active chromophores such as Disperse Red 19, a pyridinium salt based dye, and 1-amino-4-nitrobenzene are covalently locked into silica networks. The resulting hybrids are soluble and offer ease of processibility in the preparation of good-optical-quality thin films. Network materials that are akin to the traditional sol−gel approach are also prepared from the monofunctional NLO chromophore DR1 and, as expected, are found to be insoluble. Physical properties of the NLO chromophore-incorporated hybrids can be tailored by changing the molar amounts of chromophores and water, and the type of chromophore. High thermal stability and glass-transition temperatures of these hybrids offer effective electric-field poling at high temperatures and long-term temporal stabilities of the second-harmonic-generation signals at room temperature and at 80 °C. The $\chi^{(2)}$ values for the networks were found to be in the range of $(1.2-37) \times 10^{-8}$ esu.

Introduction

There is continued interest in the search for efficient second-order nonlinear optical (NLO) materials because of their potential applications in photonics-based technologies for optical telecommunication, information processing, and data storage.[1−4] Several chemical methodologies such as self-assembled thin films, functionalized polymers, and organic−inorganic composites have been developed to meet device-oriented requirements. The latter include high mechanical and dimensional stability, low optical loss, high thermal stability, adequate number density of acentrically aligned high-β chromophores, long-term temporal stability of the second-order NLO signals, etc.[2−4] Recently, organic−inorganic hybrid materials, prepared through sol−gel processing, have received much attention because of the inherent properties of the silica matrix.[5−10] The physical properties of these hybrid materials address most of the important issues related to practical-device fabrication for example, thermal endurance during electric-field poling for chromophore alignment, low optical loss, and high temporal stability of the NLO signal that is attributed to their high-glass-transition temperatures. In addition, thin films of the inorganic network materials can avoid or greatly reduce surface damage induced by corona discharge poling, which is a serious problem in poled organic polymer based thin films.[11]

There are two different types of sol−gel composites that have been extensively used in the past. In these, organic NLO chromophores can be either physically blended with the silica network or chemically bound to tri(alkoxy)silanes before hydrolytic condensation.[5,6] In the former, the performance is limited by the chromophore concentration usually to a maximum of 15−20 wt % as a result of phase separation, sublimation at an elevated temperature during electric-field poling, and thermal and environmental instability. Some of these problems can be resolved through the latter process, in which chemical attachment of the chromophore prevents it from aggregating, and one can achieve an adequate chromophore density for enhancing optical nonlinearity and improve thermal stability.[6] In addition, better elasticity imparted by the organic chromophores in the stiff SiO_2 backbones prevents the formation of cracks during fabrication of thin films.[12]

Traditionally, sol−gel-derived chromophore-bound materials are prepared by linking NLO molecules to tri(methoxy or

* To whom correspondence should be addressed. Tel.: 514-398-6912. Fax: 514-398-3797. E-mail: ashok_kakkar@maclan.mcgill.ca.

(1) Hornak, L. A. *Polymers for Lightwave and Integrated Optics*; Marcel Dekker: New York, 1992.

(2) Marks, T. J.; Ratner, M. A. *Angew. Chem., Int. Ed. Engl.* **1995**, *34*(2), 155.

(3) Burland, D. M.; Miller, R. D.; Walsh, C. A. *Chem. Rev.* **1994**, *94*, 31.

(4) (a) Nalwa, H. S.; Watanabe, T.; Miyata, S. in *Nonlinear Optics of Organic Molecules and Polymers*; Nalwa, H. S., Miyata, S., Eds.; CRC Press: Boca Raton, 1997; 89. (b) Zyss, J. in *Nonlinear Optical Properties of Organic Molecules & Crystals*; Chemla, D. S., Zyss, J., Eds.; Academic Press: Orlando, 1987.

(5) (a) Klein, L. C. *Sol−Gel Optics, Processing and Applications*; Kluwer Academic Press: Boston, 1994. (b) Brinker, C. J.; Scherer, G. W. *Sol−Gel Science*; Academic Press: New York, 1989.

(6) (a) Brinker, C. J.; Scherer, G. W. *Sol−Gel Science*; Academic Press: Boston, 1990. (b) Pope, E. J. A.; Sakka, S.; Klein, L. C. *Sol−Gel Science and Technology*; American Ceramic Society: Westerville, 1995.

(7) (a) Hill, R. A.; Knoesen, A.; Mortazavi, M. A. *Appl. Phys. Lett.* **1994**, *65*, 1733. (b) Zhang, Y.; Prasad, N.; Burzynski, R. *Chem. Mater.* **1992**, *4*, 851. (c) Jeng, R. J.; Chen, Y. M.; Jain, A. K.; Kumar, J.; Tripathy, S. K. *Chem. Mater.* **1992**, *4*, 972. (d) Marturunkakul, S.; Chen, J. I.; Jeng, R. J.; Sengupta, S.; Kumar, J.; Tripathy, S. K. *Chem. Mater.* **1993**, *5*, 743.

(8) Mark, J. E.; Lee, C.; Biancon, P. A. *Hybrid Organic−Inorganic Composites*; ACS Symposium Series 585; American Chemical Society: Washington, DC, 1995.

(9) Min, Y. H.; Lee, K. S.; Youn, C. S.; Do, L. M. *J. Mater. Chem.* **1998**, *8*, 1225.

(10) Haruvy, Y.; Webber, S. *Chem. Mater.* **1991**, *3*, 501.

(11) Hill, R. A.; Knoesen, A.; Mortazavi, M. A. *Appl. Phys. Lett.* **1994**, *65*, 1733.

(12) Schmidt, H. *J. Non-Cryst. Solids* **1989**, *112*, 379.

10.1021/ja983274j CCC: $18.00
Published on Web 03/31/1999

ethoxy)silane followed by hydrolysis and condensation to form an amorphous silica network.[6−8] The hydrolytic condensation, in general, needs to be catalyzed using an acid or a base or under neutral conditions using fluoride anions at elevated temperatures.[7] The resulting cross-linked matrixes are similar, in their mode of attachment of the NLO chromophore, to the side chain tethered linear polymers and are insoluble in common organic solvents. Therefore, a precursor generated from the hydrolysis of trialkoxysilanes has to be used to cast thin films. The latter are subsequently thermally cured to form a network on the substrate, which lowers optical quality of the thin film.[5,7,8] The precursor employed in the construction of the thin films is usually an oligomer with very low viscosity, which causes serious problems in preparing uniform thin films. The structural control of the matrixes is dependent on a number of factors including the type of catalyst used to enhance the reactivity of Si−OR groups, the pH of the reaction mixture, which controls the degree of condensation, and the temperature.[5,6] In addition, reaction rates can be diminished by the presence of byproducts such as methanol or ethanol.[9]

We describe herein an alternative route based on simple acid−base hydrolytic chemistry[13−15] of readily available aminosilanes, e.g., tetra(diethylamino)silane ($Si(NEt_2)_4$) with NLO active molecules containing terminal OH groups and H_2O, to synthesize NLO chromophore bound organic−inorganic hybrid materials. This synthetic approach is similar, in principle, to the traditional sol−gel technique, but requires milder reaction conditions without the use of catalysts to facilitate the hydrolysis/condensation reaction sequence. To demonstrate the versatility of this approach, two different types of NLO chromophores[16] with (i) bifunctional end groups, such as 2,2′-[4-[(4-nitrophenyl)-azo]phenyl]aminobis(ethanol) [$(HO(CH_2)_2)_2NC_6H_4N{=}NC_6H_4NO_2$] Disperse Red 19 (**1a**), pyridinium salt based dye, 1-methyl-4−4′-[*N*,*N*-bis(2-hydroxyethyl)amino]styryl}pyridinium tetraphenylborate [$(HO(CH_2)_2)_2NC_6H_4C{=}CC_6H_5N{-}CH_3]B(C_6H_5)_4$ (**1b**), and 1-bis(3-hydroxypropyl)amino-4-nitrobenzene [$(HO(CH_2)_3)_2NC_6H_4NO_2$] (**1c**), and (ii) monofunctional end groups, such as Disperse Red 1 (DR1) [$(C_2H_5)(HO(CH_2)_2)NC_6H_4N{=}NC_6H_4NO_2$], were employed for this study. The synthesis of NLO active hybrids using DR1 bears close resemblance to the traditional sol−gel technique, and as expected, the resulting matrixes are insoluble in common organic solvents. However, network materials synthesized using bifunctional chromophores are found to be soluble in polar solvents. The latter hybrid materials contain matrix-incorporated NLO active chromophores that are essentially sandwiched in a siloxane-based network, as compared to the traditional sol−gel approach, in which NLO chromophores are tethered to the surface. By controlling the amount of $Si(NEt_2)_4$ and water used in hydrolysis and reaction temperatures and by changing the NLO-chromophores, important physical characteristics of these hybrid materials, including solubility and glass-transition temperatures, can be tailored. The NLO properties of the networks were investigated by using the second-harmonic generation (SHG) technique, and the $\chi^{(2)}$ values were found to be in the range of $(1.2-37) \times 10^{-8}$ esu. The SHG signals exhibited long-term stabilities at room temperature and at 80 °C. The latter can be attributed to high thermal stabilities and glass-transition temperatures of the hybrid materials. These cross-linked siloxane networks containing sandwiched high-β chromophores in the backbone that can be isolated as soluble powders offer substantial advantages in constructing thin-film-based acentric materials with large and stable bulk $\chi^{(2)}$ as well as optical clarity.[2−4]

Scheme 1

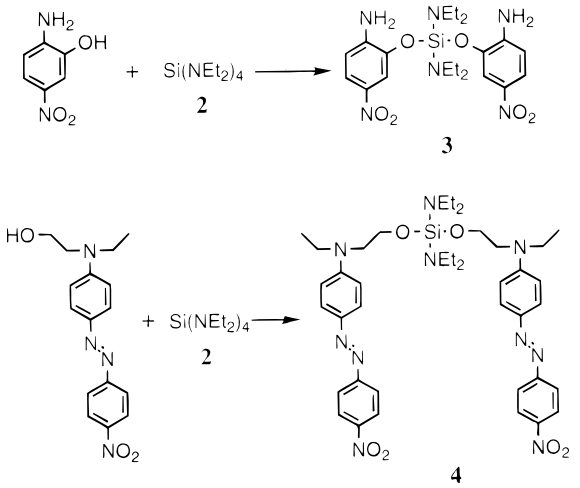

Results and Discussion

Synthesis. It is well known that aminosilanes (R_3Si-NR_2, R = Me, Et), which can be easily prepared from the reaction of the corresponding chlorosilanes with excess amines, react quantitatively with organic compounds containing acidic protons via acid−base hydrolysis.[13−15] For example, organic chromophores **1a**−**c** and Disperse Red 1 (DR1), which contain terminal OH groups, react with trimethylsilyldiethylamine, $Me_3Si-NEt_2$, to yield the corresponding silylated compounds and diethylamine. In a similar reaction, it is interesting to note that the hydrolysis of one equivalent of $Si(NEt_2)_4$ with 4 equiv of 2-amino-5-nitrophenol does not yield a tetrasubstituted silane, as expected, but produces a dimer (**3**) (Scheme 1). The ^{1}H NMR spectrum of **3** confirm that there are two diethylamino groups on silicon in the dimer. The peaks due to these diethylamino groups disappear when dimer **3** is hydrolyzed by water molecules, and a new peak due to the hydroxyl proton on silicon (Si−OH) appear at 9.37 ppm. The formation of dimer **3** can be explained by considering the steric bulk of the organic chromophore. When two amino groups (NEt_2) on silicon are replaced with two bulky organic fragments, the crowding around silicon prevents further substitution of two more NEt_2 groups on silicon. Similarly, the reaction between $Si(NEt_2)_4$ and DR1 gives DR1 based dimer **4** with two amino groups still on silicon (Scheme 1). In the ^{1}H NMR spectrum of **4**, the peak from the methylene protons adjacent to the hydroxyl group shifts from 3.52 to 3.85 ppm when its oxygen is covalently attached to silicon in the dimer.

Using a similar acid−base hydrolytic chemistry approach to that described above, soluble hybrid materials were prepared by linking bifunctional NLO chromophores containing two terminal OH groups, Disperse Red 19 (**1a**), 1-methyl-4,4′-[*N*,*N*-bis(2-hydroxyethyl)amino]styryl pyridinium tetraphenylborate (**1b**), or 1-bis(3-hydroxypropyl)amino-4-nitrobenzene (**1c**) with $Si(NEt_2)_4$, followed by hydrolysis with varying amounts of water and then condensation (Scheme 2). For example, hybrid **5a** was

(13) Jiang, H.; Kakkar, A. K.; Lebuis, A.-M.; Zhou, H.; Wong, G. K. *J. Mater. Chem.* **1996**, *6*, 1075.
(14) (a) Jiang, H.; Kakkar, A. K. *Macromolecules* **1998**, *31*(8), 2501. (b) Jiang, H.; Kakkar, A. K. *Macromolecules* **1998**, *31*(13), 4170.
(15) Jiang, H.; Kakkar, A. K. *Adv. Mater.* (*Weinheim, Ger.*) **1998**, *10*, 1093.
(16) (a) Moon, K.-J.; Shim, H.-K.; Lee, K.-S.; Zieba, J.; Prasad, P. N. *Macromolecules* **1996**, *29*, 861. (b) Wang, N. P.; Leslie, T. M.; Wang, S.; Kowel, S. T. *Chem. Mater.* **1995**, *7*, 185. (c) Chen, M.; Yu, L.; Dalton, L. R.; Shi, Y.; Steier, W. H. *Macromolecules* **1991**, *24*, 5421. (d) Anderson, H. H. *J. Am. Chem. Soc.* **1952**, *74*, 1421.

Scheme 2

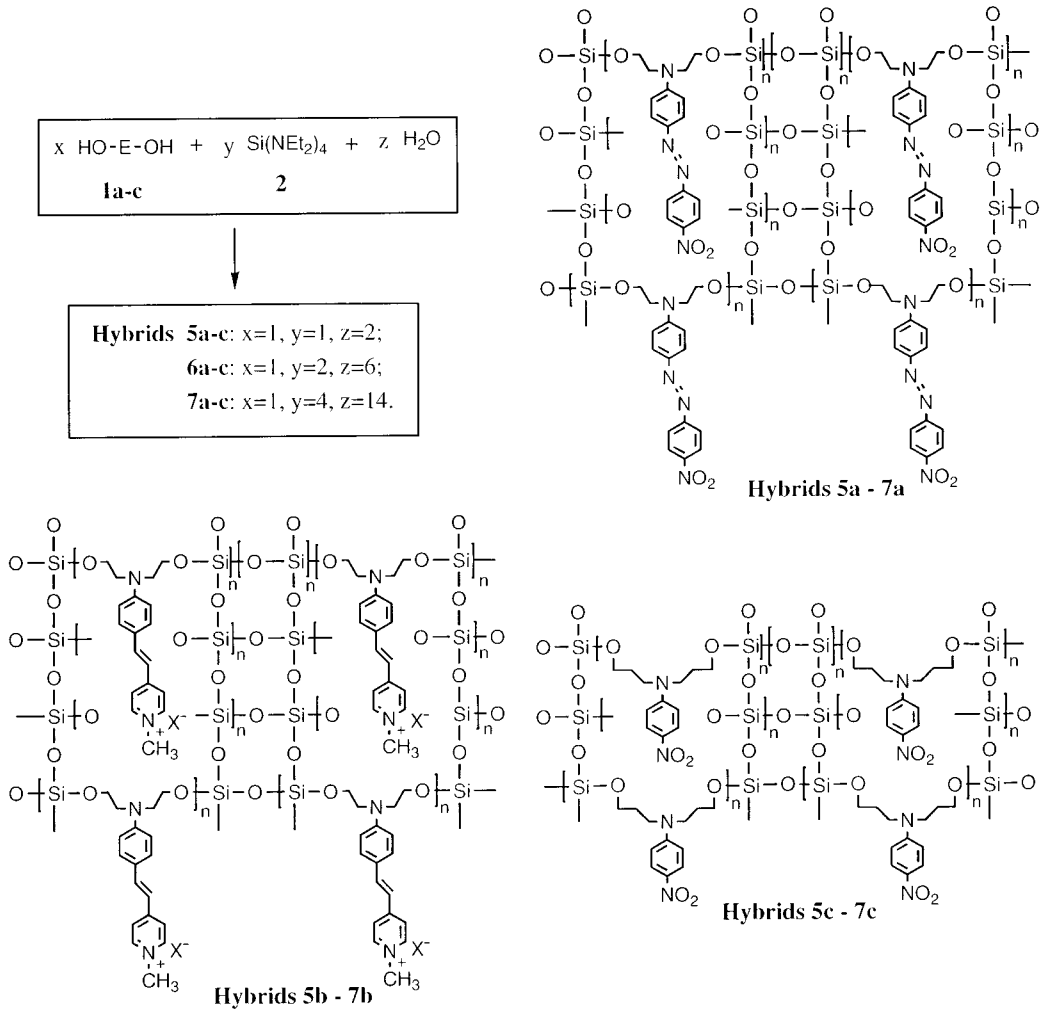

synthesized by first reacting equimolar quantities of Disperse Red 19 and $Si(NEt_2)_4$ at room temperature for 4h. Then, 2 equiv of water molecules were added to hydrolyze the remaining amino groups on silicon and this was followed by condensation at an elevated temperature to generate a cross-linked-silica network. The basicity of the $Si-NEt_2$ bond is higher than the Si−OR bond of $XSi(OR)_3$ species (R = Me, Et) used in the traditional sol−gel technique, and its hydrolysis with chromophores containing terminal OH groups of the chromophores and H_2O is much more facile and does not require any catalyst. Condensation of the resulting Si−OH groups has been shown to be catalyzed by bases such as amines.[17] In the methodology described in Scheme 2, the hydrolysis of $Si(NEt_2)_4$ produces diethylamine (a potential catalyst) as a byproduct. In the traditional sol−gel processing, hydrolysis of $-Si(OR)_3$ affords either methanol or ethanol as a side product, both of which have been demonstrated to diminish hydrolytic condensation reactions.[6]

The extent of cross-linkages in the hybrid materials was controlled by varying the molar amounts of $Si(NEt_2)_4$ and water in the reaction mixture. Hybrids **6a**−**c** and **7a**−**c**, which are expected to be more cross-linked than **5a**−**c**, were prepared by changing the molar ratio of chromophore/$Si(NEt_2)_4$/water from 1:2:6 to 1:4:14, respectively. The synthesis of these hybrids was monitored by ^{1}H NMR and solid-state ^{13}C NMR. The peak around 4.4 ppm for the hydroxyl group of the organic chromophore disappeared in the ^{1}H NMR spectra upon network formation and that from the CH_2 group adjacent to the oxygen atom shifted from ∼3.1 ppm to ∼3.5 ppm and from 3.1 ppm to ∼3.7 ppm for CH_2 adjacent to the nitrogen atom. The chemical shift in the ^{13}C NMR spectra for the methylene carbon adjacent to the hydroxyl group moved from ∼58 ppm to ∼62 ppm when its oxygen was covalently bound to silicon.

For a comparison between the networks prepared using the traditional sol−gel approach and those from bifunctional chromophores using our acid−base hydrolytic chemistry, an NLO chromophore containing only one terminal OH group, Disperse Red 1 (DR1), was also employed for the synthesis of cross-linked hybrid materials (Scheme 3). Hybrid **8** was synthesized by first reacting equimolar quantities of DR1 and tetra(diethylamino)silane at room temperature. Tri(diethylamino)silane containing the DR1 terminated fragment, thus obtained as a sol−gel precursor, is similar to tri(alkoxy)silanes used in traditional sol−gel processing,[6] except for the amino groups on silicon that are more basic and more easily hydrolyzed than alkoxides. Three molar equivalents of water were then added, followed by condensation at an elevated temperature to form the chromophore-bound silica network. Compared with the traditional sol−gel route, the chemistry described in Scheme 3 requires milder reaction conditions as a result of the higher basicity of $Si-NEt_2$, and it is not necessary to add any additional

(17) (a) Glaser, R. H.; Wilkes, G. L.; Bronnimann, C. E. *J. Non-Cryst. Solids* **1989**, *113*, 73; (b) Suratwala, T.; Gardlund, Z.; Davidson, K.; Uhlmann, D. R.; Watson, J.; Bonilla, S.; Peyghambarian, N. *Chem. Mater.* **1998**, *10*, 199.

Scheme 3

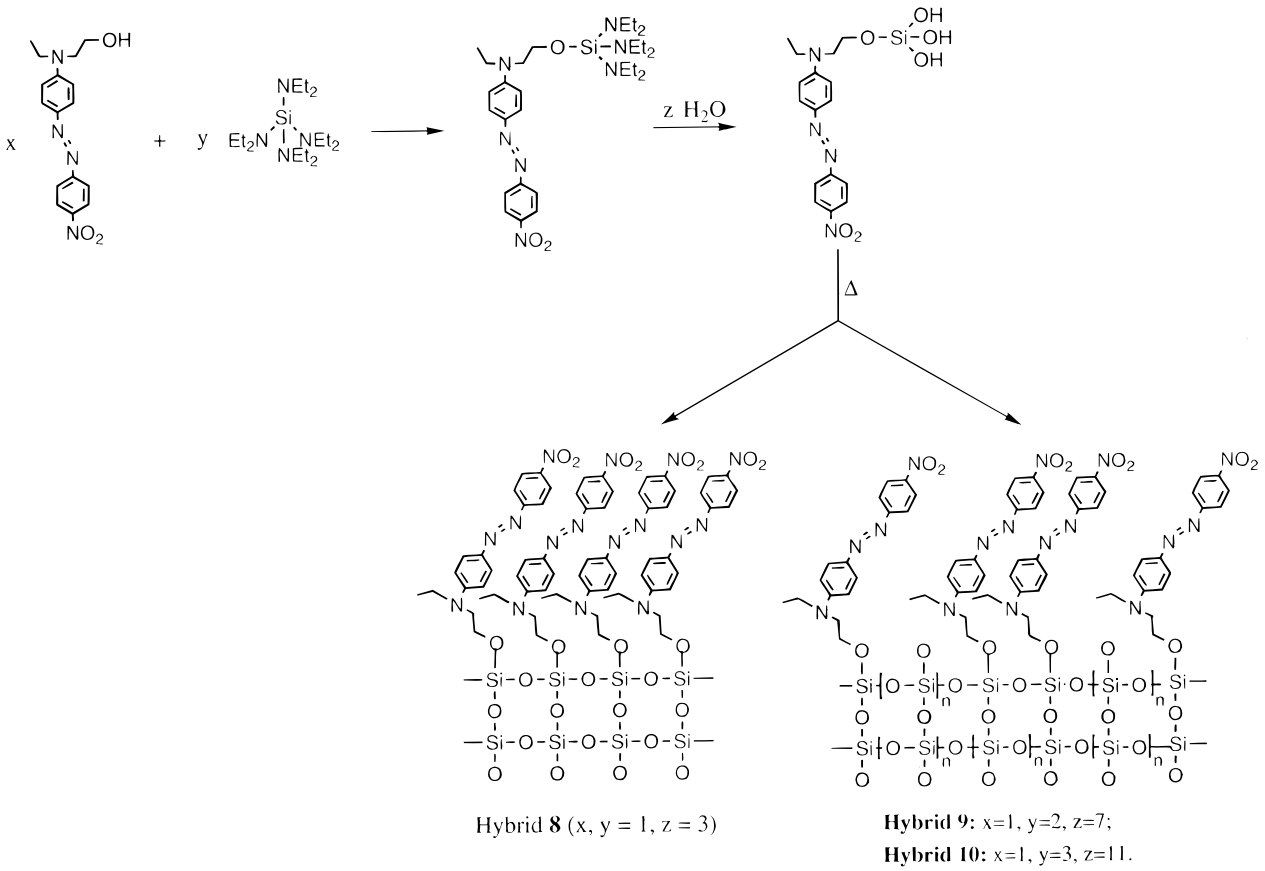

catalyst to facilitate condensation reactions, since diethylamine (a potential catalyst) is generated as a byproduct. Hybrids **9** and **10** were prepared using a similar approach, but by increasing the molar amount of $Si(NEt_2)_4$ in the reaction from 1 equiv, for hybrid **8**, to 2 for hybrid **9** and 3 for hybrid **10**, while keeping the amount of organic chromophore constant.

Hybrids **5**−**7**, prepared from bifunctional chromophores, were found to be soluble in polar solvents, such as *N*-methylpyrrolidinone (NMP) and dimethyl sulfoxide (DMSO), while hybrids **8**−**10**, synthesized using monofunctional chromophores, were insoluble. This difference in solubility may be attributed to the presence of partly linear siloxane-linked chains in the silica matrix of hybrids **5**−**7**. For hybrids **8**−**10**, synthesized from chromophore-terminated tri(amino)silanes, there is no possibility for such linear chains to be formed in the silica matrix. A quantitative estimation of the solubility of these materials was carried out by dissolving a given amount of the hybrid into a fixed amount of the solvent, and it was found to be in the order **5** > **6** > **7**. The latter can be understood by considering the amount of cross-linked components in the network. As the molar amounts of $Si(NEt_2)_4$ and water molecules are increased in the reaction, the extent of cross-linking by hydrolytic condensation increases, leading to lower solubility and higher molecular weight (see below).

The molecular weights of the hybrids were estimated by viscosity measurements which were carried out by using a Ubblelohde type viscometer and NMP as the solvent. Since hybrids **8**−**10** are insoluble, there is no viscosity data reported for these materials. As seen from Table 1, for hybrids which contain similar organic chromophores, the viscosity was found to be in a decreasing order of **7** > **6** > **5**. This implies that the molecular weights of the networks (estimated to be in the range of ∼10 000−20 000) also decrease in the same order.

Table 1. Physical Properties of Hybrid Materials

hybrid	η_{int}, dL/g	λ_{max} (nm)	T_d (°C)	T_g (°C)
5a	0.12	480	314	155
6a	0.14	480	349	182
7a	0.17	481	360	224
5b	0.10	472	242	148
6b	0.11	472	263	279
7b	0.15	472	246	227
5c	0.13	398	319	124
6c	0.11	398	346	151
7c	0.15	398	331	197
8		484	347	254
9		484	372	273
10		483	365	297

[a] T_d = Decomposition temperature where there is 5% weight loss under nitrogen. [b] T_g = Glass transition temperature.

^{29}Si NMR Spectra. Solid-state ^{29}Si NMR spectroscopy is a valuable technique for examining the structure of silica based network materials.[17] There are four possible structures of siloxane linkages in these hybrids with characteristic ^{29}Si NMR chemical shifts. The Q^4 type of Si−O units represent a silicon bound to four other silicon atoms through oxygen bridges and appear at approximately −110 to −112 ppm; Q^3 represents silicon bound to three other silicon atoms through oxygen bridges and one R group, where R = H or E in Scheme 2, −100 to −102 ppm; Q^2 represents silicon bound to two other silicon atoms through oxygen bridges and two R groups, −90 to −94 ppm; and Q^1 represents silicon bound to another silicon atom through oxygen and three R groups, −80 to 85 ppm.[17]

Hybrid **5a** showed four peaks in its cross-polarized solid-state ^{29}Si NMR spectra that can be assigned to tetrafunctional Si−O units of Q^4 (−111.3 ppm), Q^3 (−101.5 ppm), Q^2 (−89.0 ppm), and Q^1 (−84.8 ppm) type, respectively. The hybrid **6a**

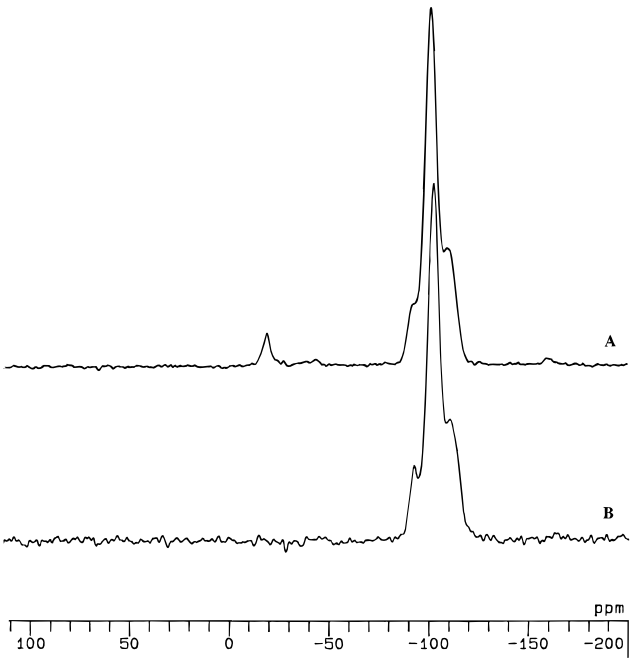

Figure 1. Solid-state ^{29}Si NMR spectra of hybrid **9** before (B) after (A) wet processing.

also showed four peaks with similar assignments as those for **5a**, −110.2 ppm (Q^4), −102.3 ppm (Q^3), −92.3 ppm (Q^2), −85.3 ppm (Q^1).[15] The peak from Q^1-type Si−O units significantly decreased in going from **5a** to **6a**, while the peaks from Q^3-type and Q^4-type Si−O units were enhanced. The peak from Q^1-type Si−O units was missing in the solid-state ^{29}Si NMR spectrum of hybrid **7a** which showed three broader peaks in the region −96.4 to −110.6 ppm with similar assignments as for hybrids **5a** and **6a**. Similar changes were also observed for the hybrids in going from **5b**, **6b** to **7b**, and from **5c**, **6c** to **7c**.

In the ^{29}Si NMR spectra of networks **8**−**10** (Figure 1), similar peak assignments as for hybrids **5**−**7** can be made hybrid **8** −85.74 (Q^1), −92.13 (Q^2), −101.72 (Q^3), −110.42 (Q^4); hybrid **9** −92.27 (Q^2), −101.85 (Q^3), −109.81 (Q^4); hybrid **10** −92.51 (Q^2), −103.08 (Q^3), −111.48 (Q^4). Upon comparing hybrids **8**−**10**, the peak from Q^1-type Si−O units is missing in **9** and **10**, and the peak intensities of Q^3- and Q^4-type Si−O units have increased. The peak intensities for Q^2-type Si−O units decreased, and almost disappeared, for hybrid **10**. These results suggest that the degree of condensation increases as we go from **5** to **7** or from **8** to **10**. This is in line with increasing molar amounts of tetra(diethylamino)silane and water used in the reaction leading to cross-linked matrixes, as discussed above.

Upon comparing ^{29}Si NMR spectra of hybrids **5**−**7** (that are synthesized from bifunctional chromophores) with those of hybrids **8**−**10** (prepared using a monofunctional chromophore), it is important to note the difference in intensity ratios of tetrafunctional Si−O units. For example, hybrids **7a** and **10** both contain Disperse Red dye based chromophores and have similar chromophore densities; however, the former displayed a much stronger peak of Q^2-type Si−O units (−92.9 ppm) than the latter. Hybrid **10** showed higher relative intensities for Q^3-type Si−O units (−103.1 ppm) and Q^4-type Si−O units (−111.5 ppm) as compared with the corresponding peaks of hybrid **7a**. These results indicate that hybrids **8**−**10**, prepared from chromophore-terminated tri(amino)silanes, are more cross-linked than hybrids **5**−**7**.

FT-IR Spectra. The siloxane-based hybrid materials show a characteristic and strong Si−O stretch in their infrared spectra in the 1000−1130 cm^{-1} region. An increase in the intensity and width of peaks usually accompanies an increase in the extent of cross-linking in the networks.[5−10] By comparing the stretching frequencies of the hybrids containing similar NLO chromophores, it was observed that the Si−O stretches became broader and more complex with the increase of molar ratio of $Si(NEt_2)_4$ in the reaction. The hybrid **5a** displayed a Si−O−Si stretch in the region 1069−1125 cm^{-1}, the hybrid **6a** displayed a broader Si−O−Si stretch in the region 1067−1139 cm^{-1}, and the hybrid **7a** produced a similar but much broader stretch than **5a** or **6a** in the region 1066−1165 cm^{-1}. Hybrids **8**−**10** prepared from a monofunctional chromophore DR1, displayed Si−O−Si stretches in the region 1075−1140 cm^{-1} (hybrid **8**), 1070−1144 cm^{-1} (hybrid **9**), and 1068−1146 cm^{-1} (hybrid **10**). Similarly, it was found that the peak width became broader in going from hybrid **8** to hybrid **10**. It is inferred from these results that, while keeping the amount of NLO chromophore constant, the larger the molar amount of $Si(NEt_2)_4$ used in the reaction, the higher the cross-linking of networks.

Thermal Stability. The stabilities of the hybrid materials at higher temperatures were determined by thermogravimetric analysis (TGA). The decomposition temperatures (T_d's), the temperatures at which 5% weight loss was observed in a nitrogen atmosphere, are reported in Table 1. The hybrid materials show high thermal stabilities due to the mechanical strength imparted by stable and strong Si−O bonds in the networks. Hybrids **5a**−**7a**, **5c**−**7c**, and **8**−**10**, which contain either **1a**, **1c** or DR1 as organic NLO chromophores, show decomposition temperatures from 314−372 °C. The latter are adequate in meeting thermal requirements in the fabrication of optical devices.[1] T_d's of hybrids **5b**−**7b** which contain pyridinium salt **1b** as the NLO chromophore are about 100 °C lower. This is probably due to lower thermal stability of the ionic salt which decomposes much faster than the siloxane backbone. T_d's of hybrids **8**−**10**, prepared from DR1, were found to be higher than those of hybrids **5a**−**7a**, prepared from DR19. For example, the thermal stability of hybrid **8** (347 °C) was 33 °C higher than that of hybrid **5a** (314 °C), and the thermal stability of hybrid **9** (372 °C) was 23 °C higher than that of **6a** (349 °C) and 12 °C higher than that of **7a** (360 °C).[15] This increase in thermal stability can be explained considering the extent of silica-network formation, which is higher in hybrids **8**−**10** than **5**−**7**.

Hydrolytic Stability of Hybrids. Since the networks **5**−**10** contain Si−OR groups, it is important to determine their stability toward water. The effect of hydrolysis on hybrid materials was explored using solid-state ^{29}Si NMR. The networks were wetted by soaking in water overnight, were filtered, and were dried under vacuum for 24 h. No change in the ^{29}Si NMR spectra of hybrids **5**−**7** was observed. However, for hybrids prepared using monofunctional chromophore DR1, for example hybrid **9**, a new peak at 19.43 ppm appeared after wet processing (Figure 1). The wetted hybrids **8**−**10** were washed repeatedly with common organic solvents, and the soluble part was identified, using ^{1}H NMR, to be chromophore, DR1. These results indicate that hybrids **5**−**7**, prepared from bifunctional chromophores, are very stable toward hydrolysis; however, the Si−OR bond attaching the DR1-terminated monofunctional chromophore to Si in hybrids **8**−**10** may be slightly sensitive to hydrolysis. This difference in stability can be understood by considering the structure of these hybrid materials. In hybrids **8**−**10**, only one side of the NLO chromophore is covalently attached to the silica network, but in hybrids **5**−**7** the NLO chromophore is embedded

into the silica backbone through both sides. The latter leads to higher water resistance of the these hybrids.

Glass-Transition Temperatures. The glass-transition temperature (T_g) is an important parameter for determining stability of the dipolar orientation of chromophores in the polymer matrix. T_g's of the hybrid materials were determined using differential scanning calorimetry, and the data are presented in Table 1. The hybrid materials display high T_g's (124−297 °C) which are mainly attributed to the cross-linked siloxane networks. The data presented in Table 1 suggest that the glass-transition temperatures of the hybrids are influenced by the following factors. (i) *Efficiency of Cross-Linking*. For hybrids **8**−**10**, the T_g's of 254, 273, and 297 °C, respectively, are about 70−100 °C higher than those for hybrids **5**−**7**. This is due to higher cross-linking via hydrolytic condensation of chromophore-terminated tri(amino)silanes in **8**−**10**. (ii) *Reactant Ratio*. For hybrids containing similar chromophores, for example, Disperse Red 19 (**1a**), T_g of hybrid **7a** is 42 °C higher than that of **6a** and 69 °C higher than that of **5a**. Once again, this rise in T_g is due to an increase in the formation of cross-linkages in the silica network, when the concentration of Si(NEt$_2$)$_4$ and water molecules in the reaction is increased.[15] Similar changes in T_g with the increase of the molar amounts of Si(NEt$_2$)$_4$ and H$_2$O were observed in **5b** (148 °C), **6b** (179 °C), and **7b** (227 °C) and **5c** (124 °C), **6c** (151 °C), and **7c** (197 °C). (iii) *Size of NLO Chromophores*. For hybrids prepared using similar molar ratios of reactants, for example, Si(NEt$_2$)$_4$/chromophore/water = 1:4:14 (**7a**−**c**), T_g's of **7a** and **7b** (224 and 227 °C, respectively) are about 30 °C higher than that of **7c** (197 °C). The latter contains a smaller chromophore (**1c**), which is easier to rotate in the matrix, compared with the larger chromophores, **1a** in **7a** and **1b** in **7b**. In addition, weaker electrostatic interactions between NLO molecules in **7c** result in less chromophore locking in the siloxane network, giving more mobility to the NLO chromophores. Similar changes in T_g's were observed upon comparing hybrids **5c** with **5a** and **5b** and **6c** with **6a** and **6b** (Table 1).

UV−Vis Spectra. An examination of the linear optical properties of the hybrid materials indicated that the peak positions in their UV−vis spectra were similar to those of the corresponding organic monomers: 481 nm for **1a**, 472 nm for **1c**, 398 nm for **1c**, and 484 nm for DR1. This suggests that the absorption characteristics of the chromophores are not affected by the hydrolytic condensation processes. For hybrids **5c**−**7c**, which contain **1c** as the NLO chromophore in the backbone, the absorption maxima are around 400 nm. The second harmonic generation (SHG) wavelength of 532 nm employed in this study is beyond their absorption regions. Thus, there should be only nonresonant contributions to SHG signal in hybrids **5c**−**7c**. However, for hybrids **5a**, **5b**, **7a**, **7b**, and **8**−**10**, which contain either **1a**, **1b**, or DR1 chromophore (absorption maxima = 472−484 nm), respectively, in the silica matrix, the SHG wavelength falls within the tail of their absorption curves, and the signals are expected to be weakly resonance-enhanced (Figure 2).

The absorption coefficients (ϵ) of the soluble hybrid materials were determined by measuring the maximum absorbance for a known concentration of the solution and were found to be in the range of (4.47−5.56) × 10^4 cm^{-1} M^{-1} for hybrids **5a**−**7a**, (6.74−7.02) × 10^4 cm^{-1} M^{-1} for **5b**−**7b**, and (1.73−1.97) × 10^4 cm^{-1} M^{-1} for **5c**−**7c**. The low values of ϵ for the latter can be attributed to their small λ_{max} and dipole moments, since ϵ is quadratically proportional to these quantities.[4b]

The absorbance of the thin films of the above hybrids decreased after electric-field poling. A representative spectrum for hybrid **7a** is shown in Figure 2. It suggests that the poling-induced alignment of chromophores is parallel to the incident light. The ordering parameter of a poled thin film is defined by $(1 - A/A_0)$, where A and A_0 are absorbances before and after poling, respectively, and it is commonly used to describe the poling efficiency.[18] The ordering parameters of these hybrids were in the range of 0.14−0.28, which suggests that these polymers are efficiently poled.

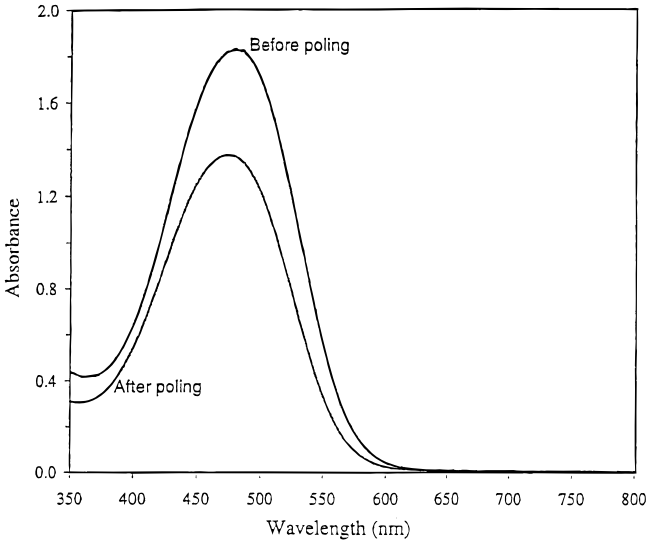

Figure 2. UV-visible absorption spectra of the thin film of the hybrid **7a** before and after electric-field poling.

Second Harmonic Generation Measurements. The second-order NLO properties of the hybrid materials were examined using the SHG technique. Thin films were spin-coated on ITO coated glass slides and then poled using a corona discharge induced electric field setup. A tungsten corona needle connected to the positive pole was kept at a 1.0-cm top-to-plane gap from the thin-film surface. The latter was grounded through the ITO-layer in contact with an aluminum plate. A Q-switched Nd:YAG laser beam, operating at 1064 nm with a pulse width of ∼10 ns and a 10-Hz repetition rate, was used as the fundamental source. The thin film was kept rotating at the speed of 2°/min from 0 to 60° during the measurement process. The SHG signal was recorded and amplified using a photomultiplier tube and then averaged in a boxcar integrator. A Y-cut quartz plate ($\chi^{(2)}$ ∼1.62 × 10^{-10} esu) was used as a reference.

Thin films of good optical quality were easily prepared for hybrids **5**−**7** because of their solubility in DMSO and NMP. For insoluble hybrids **8**−**10**, thin films were spin-coated before condensation. The pristine films consisted of low molecular weight oligomers so that chromophore orientation could be achieved at low temperatures (120−140 °C), and the silica networks with dipolar alignments of NLO chromophores were obtained on the substrates during electric-field poling.

Poling conditions and SHG characteristics of the hybrids are listed in Table 2. Poling temperatures for the thin films of hybrids **5**−**7** were set around their T_g's, for example, 170−230 °C for hybrids **5a**−**7a**. The dc electric field applied to the thin films of hybrids **8**−**10** was 4.2 kV, and that applied to the thin films of hybrids **5a**−**7a** was 4.0 kV. Thin films of hybrids **5b**−**7b** required a slightly higher electric field (4.5 kV), which may be due to the difficulty of poling salt-based chromophores. Hybrids **5c**−**7c** required only 3.5 kV, which was the lowest of the electric fields applied. Easy poling of the thin films of **5c**−

(18) Page, R. H.; Jurich, M. C.; Reck, B.; Sen, A.; Twieg, R. J.; Swalen, J. D.; Bjorlund, G. C.; Wilson, C. G. *J. Opt. Soc. Am. B* **1990**, *7*, 1239.

Table 2. Second-Order NLO Related Properties of Hybrids and Their Thin Films

hybrid	sample thickness (mm)	chromophore density (wt %)	$\chi^{(2)} \times 10^{-8}$ (esu)	poling temperature (°C)	DC electric field (kV)
5a	0.72	74	14	170	4.0
6a	0.65	65	15	190	4.0
7a	0.52	58	23	230	4.0
5b	0.90	84	17	160	4.5
6b	0.45	79	25	190	4.5
7b	0.52	67	21	230	4.5
5c	0.85	70	1.2	150	3.5
6c	0.70	61	1.8	180	3.5
7c	0.64	46	4.3	200	3.5
8	0.42	79	14	120	4.2
9	0.52	69	21	140	4.2
10	0.55	61	37	140	4.2

7c may be attributed to weaker static electric interaction among chromophores. It is interesting to note that the tetra(diethylamino)silane-based sol−gel approach leads to higher chromophore densities in the resulting hybrid materials (46−84 wt %) as compared with the traditional sol−gel methodology.[7,8]

The $\chi^{(2)}$ values were found to be in the range of $(1.2-4.4) \times 10^{-8}$ esu for **5c**, **6c**, and **7c** and $\sim(14-37) \times 10^{-8}$ esu for the other hybrids. Approximately a one order-of-magnitude difference in $\chi^{(2)}$ in these hybrids is most probably due to different molecular hyperpolarizabilities (β) of the NLO chromophores. In general, a material which contains higher β chromophores is expected to give a larger $\chi^{(2)}$ value. For example, β of disperse red dye, 59.4×10^{-30} esu, is about six times higher than that of *p*-nitroaminobenzene, 10.3×10^{-30} esu.[19]

As shown in Table 2, $\chi^{(2)}$ decreases with an increase of the chromophore density in the material. This could probably be due to a number of factors including chromophore crowding, which may reduce the strength of an applied electric field acting on each chromophore, i.e., lead to lower resultant local factors, phase separation, and the formation of centrosymmetric molecular aggregates at high concentrations. The $\chi^{(2)}$ values for hybrids **5**−**10** are somewhat lower as compared with those reported in the literature for polyimides,[16,20] polysiloxanes,[14a] and poly(imide-siloxane)s,[14b] containing covalently linked Disperse Red dyes in the main chain. The reduction of $\chi^{(2)}$ in sol−gel materials may largely be attributed to the low mobility of the chromophores in the siloxane cross-linked networks which makes efficient poling of such matrixes difficult. In addition, since NLO chromophores have a random distribution in these hybrids, it is possible that only some percentage of them can be effectively aligned by electric-field poling.

The stability of the second harmonic generation response after the removal of the external electric field was examined by monitoring the change in SHG signal intensity with time. At room temperature, there was no decay in intensity for all the hybrids (except **5c**) for the 60 days measurements were taken. Approximately 25% of the SHG signal decay was observed for **5c** over a period of 45 days. No decay in the SHG signal intensity for hybrids **7a**−**c** and **10** was observed at 80 °C measured throughout the 35 days measurements were taken (Figure 3). The long-term stabilities of SHG signals at room temperature and 80 °C can be attributed to the high T_g's of these materials.

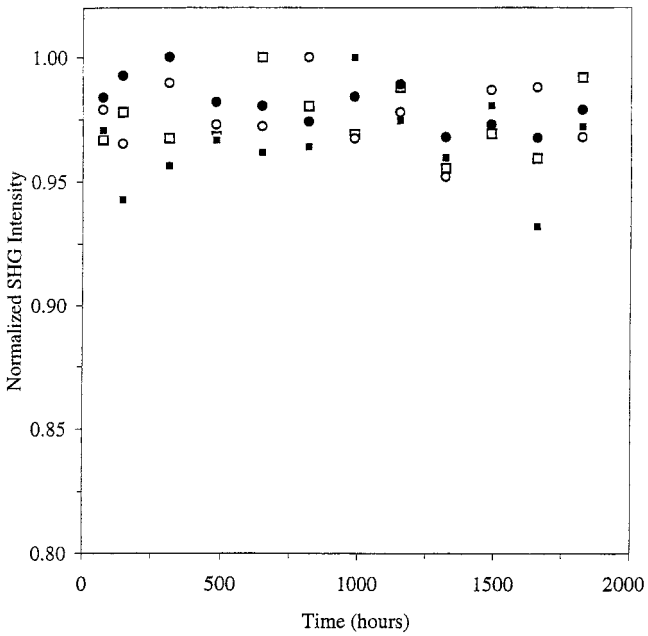

Figure 3. Temporal stability of the SHG signal from the poled thin films of **7a**, **7b**, **7c**, and **10** at 80 °C after the electric field was removed.

The thermal endurance of the SHG signal was examined by heating the thin films to 100 °C quickly first, and then the heating rate was reduced slowly and kept at 3 °C/min after 130 °C. It was observed that the SHG signal remained stable before ~180 °C, after which it started to decay slowly. When the samples were heated to 200 °C, the SHG signal decayed very fast and then completely disappeared at 215 °C (T_g of **7a**). These results are consistent with the DSC data reported in Table 1, and a similar temperature dependence of SHG signals has been observed for functionalized polyimides.[16,20]

Conclusions

Network materials in which NLO active chromophores, with either one or two terminal OH groups that are covalently bound on or in the silica matrix, have been synthesized using acid−base hydrolytic chemistry of easily accessible reagents. The new technique is similar, in principle, to the traditional sol−gel methodology, but has numerous advantages including milder reaction conditions without requiring any additional catalyst to facilitate the hydrolysis and condensation processes. As in the traditional sol−gel approach, the monofunctional chromophores yield insoluble materials that require processing of the thin films from the precursors on the substrates. However, the matrix-incorporated hybrids prepared from the bifunctional chromophores are isolated as powders that are soluble in highly polar solvents. Our results suggest that acid−base hydrolytic chemistry is a simple, highly flexible, and versatile approach to synthesizing network materials that have a unique combination of useful physical properties such as high thermal stabilities and glass-transition temperatures, which can be attributed to the degree of cross-linked siloxane networks, and desired solubility that is essential in fabricating thin films of good optical quality. The efficiently poled thin films of the hybrids show excellent second harmonic generation characteristics with high temporal stabilities of the SHG signals at room temperature and at 80 °C.

(19) Ulman, A.; Willand, C. S.; Kohler, W.; Robello, D. R.; Willams, D. J.; Handley, L. *Materials for Nonlinear Optics: Chemical Perspective*; Marder, S. R., Sohn, J. E., Stucky, G. D., Eds.; ACS Symp. Ser. 455; American Chemical Society: Washington, DC, 1991.

(20) (a) Yu, D.; Gharavi, A.; Yu, L. *J. Am. Chem. Soc.* **1995**, *117*, 11680. (b) Becker, M. W.; Sapochak, L. S.; Ghosen, R.; Xu, C.; Dalton, L. R.; Shi, Y.; Steier, W. H.; Jen, A. K.-Y. *Chem. Mater.* **1994**, *6*, 104. (c) Dalton, L. R.; Wu, B.; Harper, A. W.; Ghosn, R.; Ra, Y.; Liang, Z.; Montgomery, R.; Kalluri, S.; Shi, Y.; Steier, W. H.; Jen, A. K.-Y. In *Polymers for Second-Order Nonlinear Optics*; Lindsay, G. A., Singer, K. D., Eds; ACS Symposium Series 601; American Chemical Society: Washington, DC, 1995. (d) Lee, H.-J.; Lee, M.-H.; Han, S. G.; Kim, H.-Y.; Ahn, J.-H.; Lee, E.-M.; Won, Y. H. *Polymer Chemistry* **1998**, *36*, 301.

Experimental Section

General. All manipulations were performed using standard Schlenk line techniques. ^{1}H NMR spectra were recorded on a JEOL 270 MHz FT-NMR spectrometer, and the ^{29}Si and ^{13}C NMR spectra were recorded on a Chemagnetic CMX 300 MHz spectrometer with high-power decoupling. The FT-IR spectra were measured on a Bruker IFS-48 spectrometer, and the UV−vis absorption spectra were obtained on a Hewlett-Packard 8453 spectrophotometer. Glass transition temperatures (T_g) were measured by differential scanning calorimetry (DSC) using a Seiko TK/DSC-220 instrument, and thermogravimetric analysis (TGA) of polymers was performed using a Seiko TK/DTA-220 instrument with a heating rate of 20 °C/min. Elemental analyses were carried out by Microanalytical Services Ltd. and Guelph Chemical Laboratories Ltd. The second-order NLO properties of spin-coated thin films of hybrids were obtained using the SHG technique in which a Q-switched Nd:YAG laser beam, operating at 1064 nm with a pulse width of ∼10 ns and a 10-Hz repetition rate, was used as the fundamental source.

Materials. *N*-Methylpyrrolidinone (NMP) was dried by vacuum distillation over phosphorus pentoxide, diethyl ether over sodium, and diethylamine over potassium hydroxide. Disperse Red 1 (DR1), [4-[(4-nitrophenyl)azo]phenyl]amino(ethyl)(ethanol) [$(C_2H_5)(HO(CH_2)_2)$-$NC_6H_4N{=}NC_6H_4NO_2$] was purified by recrystallization from ethanol. All other starting materials were purchased from Aldrich and used without purification unless otherwise noted. Compounds **1a**−**c**, 2,2′-[4-[(4-nitrophenyl)azo]phenyl]aminobis(ethanol) [$(HO(CH_2)_2)_2NC_6$-$H_4N{=}NC_6H_4NO_2$] (Disperse Red 19), 1-methyl-4−4′-[*N*,*N*-bis(2-hydroxyethyl)amino]styryl}pyridinium tetraphenylborate [$(HO(CH_2)_2)_2NC_6H_4$-$C{=}CC_6H_5NCH_3]B(C_6H_5)_4$, and 1-bis(3-hydroxypropyl)amino-4-nitrobenzene [$(HO(CH_2)_3)_2NC_6H_4NO_2$], respectively, and tetra(diethylamino)silane ($Si(NEt_2)_4$ (**2**)) were prepared according to the literature procedures.[16]

Compound 3. To a solution of 2-amino-5-nitrophenol (208 mg, 2 mmol) in 40 mL of toluene was added tetra(diethylamino)silane (**2**, 180 mg, 0.5 mmol) in 5 mL of NMP dropwise. The mixture was stirred under nitrogen for 4 h and then heated to 100 °C for another 16 h. The solvent was removed under vacuum at 60 °C for 24 h. The remaining residue was washed with diethyl ether (2 × 50 mL), collected by filtration, and then dried under vacuum at 60 °C for 24 h. Yield: 310 mg, 80%. ^{1}H NMR (DMSO, ppm): δ 1.22 (t, 12H, CH_3, J_{H-H} = 5.1 Hz), 2.90 (m, 8H, N−CH_2), 6.39 (s, 4H, NH_2), 7.60 (d, 2H, C_6H_3, J_{H-H} = 8.6 Hz), 7.71 (d, 2H, C_6H_3, J_{H-H} = 8.5 Hz), 7.76 (d, 2H, C_6H_3, J_{H-H} = 8.6 Hz). Mass (MALDI-TOF): 368 ($((C_6H_5N_2O_3)_2Si(OH)_2$). UV−vis ($CHCl_3$): λ_{max}/nm 396.

Compound 4. To a solution of Disperse Red 1 (314 mg, 1 mmol) in 25 mL of anhydrous NMP, tetra(diethylamino)silane (**2**, 90 mg, 0.25 mmol) in 5 mL of NMP was added dropwise. The resulting mixture was stirred under nitrogen for 2 h and then heated to 100 °C for another 15 h. The solvent and diethylamine were removed under vacuum at 60 °C. The remaining residue was washed with diethyl ether (2 × 50 mL), collected by filtration, and then dried under vacuum at 60 °C for 24 h. Yield: 320 mg, 81%. ^{1}H NMR (DMSO, ppm): δ 1.18 (t, 6H, CH_3, J_{H-H} = 6.0 Hz), 1.24 (t, 12H, CH_3, J_{H-H} = 5.5 Hz), 2.96 (m, 8H, NCH_2), 3.52 (m, 4H, NCH_2), 3.60 (t, 4H, NCH_2, J_{H-H} = 6.2 Hz), 3.85 (t, 4H, OCH_2, J_{H-H} = 6.2 Hz), 6.47 (d, 4H, C_6H_4, J_{H-H} = 8.8 Hz), 7.79 (d, 4H, C_6H_6, J_{H-H} = 8.8 Hz), 7.98 (d, 4H, C_6H_4, J_{H-H} = 8.8 Hz), 8.17 (d, 8H, C_6H_4, J_{H-H} = 8.8 Hz). Mass (MALDI-TOF): 688 ($((C_{16}H_{17}N_4O_3)_2Si(OH)_2$). UV−vis ($CHCl_3$): λ_{max}/nm 481.

A common procedure for synthesizing hybrids **5**−**7** is outlined below.

Hybrid 5a. To a solution of Disperse Red 19 (**1a**, 660 mg, 2 mmol) in 30 mL of anhydrous NMP was added tetra(diethylamino)silane (**2**, 632 mg, 2 mmol) in 10 mL of NMP dropwise under nitrogen. The resulting mixture was stirred at room temperature for 4 h, and then a suitable amount of water (72 mg, 4 mmol) was added. The resulting mixture was heated to 80 °C for another 24 h. The solvent was reduced to half its volume under vacuum at 70 °C. The remaining mixture was poured into methanol. The precipitate was collected by filtration. The product was washed with methanol several times and dried under vacuum at 70 °C for 24 h (620 mg, 82%). ^{1}H NMR (DMSO, ppm): δ 3.61 (t, 4H, OCH_2, J_{H-H} = 5.6 Hz), 3.71 (t, 4H, NCH_2, J_{H-H} = 5.6 Hz), 6.90 (d, 2H, C_6H_4, J_{H-H} = 8.8 Hz), 7.84 (d, 2H, C_6H_4, J_{H-H} = 8.7 Hz), 7.93 (d, 2H, C_6H_4, J_{H-H} = 8.7 Hz), 8.35 (d, 2H, C_6H_4, J_{H-H} = 8.8 Hz), 9.37 (SiOH). ^{29}Si NMR (solid-state, ppm): δ −84.76 (Q^1), −88.93 (Q^2), −101.46 (Q^3), −111.28 (Q^4). ^{13}C NMR (solid state, ppm): δ 52.65 (NCH_2), 61.12 (OCH_2), 112.79 (C_6H_4), 118.27 (C_6H_4), 125.08 (C_6H_4), 131.41 (C_6H_4), 136.80 ($C_6H_4N{=}N-$), 147.08 (C_6H_4-NO_2), 152.40 ($C_6H_4NR_2$), 155.58 ($C_6H_4N{=}N-$). FT-IR (KBr, cm^{-1}): 1069−1125 (SiO). UV−vis (NMP) λ_{max}/nm 480 (ϵ = 55 600 cm^{-1} M^{-1}). Anal. Calcd for $C_{16}H_{16}N_4O_6Si$(388): C, 49.49; H, 4.12; N, 14.43. Found: C, 50.34; H, 4.69; N, 15.27.

Hybrid 5b. Yield: 80%. ^{1}H NMR (DMSO, ppm): δ 3.61 (d, 4H, OCH_2, J_{H-H} = 5.4 Hz), 3.73 (d, 4H, NCH_2, J_{H-H} = 5.4 Hz), 4.20 (s, 3H, N^+CH_3), 6.4−7.3 (br, 23H, C_6H_4, BC_6H_5 and ═CH), 7.60 (d, 2H, C_6H_4, J_{H-H} = 8.8 Hz), 7.92 (d, 1H, ═CH, J_{H-H} = 15.8 Hz), 8.04 (d, 2H, C_6H_4, J_{H-H} = 8.8 Hz), 8.71 (d, 2H, C_6H_4, J_{H-H} = 8.8 Hz), 9.37 (SiOH). ^{29}Si NMR (solid-state, ppm): δ −85.12 (Q^1), −90.42 (Q^2), −101.25 (Q^3), −110.48 (Q^4). ^{13}C NMR (solid-state, ppm): δ 45.81 (CH_3), 54.29 (NCH_2), 61.74 (OCH_2), 113.56 (C_6H_4), 117.87 (C_6H_4), 120−131 (C_6H_4, −CH═CH−), 135.69 (C_6H_4), 142.45 ($C_6H_4C{=}C-$), 149.50 ($C_6H_4C{=}C-$), 153.07 ($C_6H_4NR_2$), 164.79 ($C_5H_4NCH_3$). FT-IR (KBr, cm^{-1}): 1072−1175 (SiO). UV−vis (NMP): λ_{max}/nm 472 (ϵ = 69 600 cm^{-1} M^{-1}). Anal. Calcd for $C_{42}H_{41}BN_2O_4Si_1$ (675.8): C, 74.58; H, 6.07; N, 4.14. Found: C, 75.68; H, 6.76; N, 3.79.

Hybrid 5c. Yield: 74%. ^{1}H NMR (DMSO, ppm): δ 1.81 (m, 4H, CH_2), 3.52 (d, 4H, OCH_2, J_{H-H} = 5.8 Hz), 3.68 (d, 4H, NCH_2, J_{H-H} = 5.8 Hz), 6.77 (d, 2H, C_6H_4, J_{H-H} = 8.9 Hz), 8.05 (d, 2H, C_6H_4, J_{H-H} = 8.9 Hz), 9.37 (SiOH). ^{29}Si NMR (solid, ppm): δ −84.46 (Q^1), −93.61 (Q^2), −101.49 (Q^3), −111.08 (Q^4). ^{13}C NMR (solid, ppm): δ 30.06 (CH_2), 50.63 (NCH_2), 60.54 (OCH_2), 109.85 (C_6H_4), 126.34 (C_6H_4), 137.39 ($C_6H_4NO_2$), 154.28 ($C_6H_4NR_2$). FT-IR (KBr, cm^{-1}): 1062−1115 (Si−O). UV−vis (NMP): λ_{max}/nm 398 (ϵ = 19 700 cm^{-1} M^{-1}). Anal. Calcd for $C_{12}H_{16}N_2O_6Si$ (476): C, 46.15; H, 5.13; N, 8.97. Found: C, 46.96; H, 5.72; N, 8.56.

Hybrid 6a. Yield: 85%. ^{1}H NMR (DMSO, ppm) δ 3.65 (t, 4H, OCH_2, J_{H-H} = 5.6 Hz), 3.77 (t, 4H, NCH_2, J_{H-H} = 5.6 Hz), 6.94 (d, 2H, C_6H_4, J_{H-H} = 8.8 Hz), 7.85 (d, 2H, C_6H_4, J_{H-H} = 8.7 Hz), 7.95 (d, 2H, C_6H_4, J_{H-H} = 8.7 Hz), 8.40 (d, 2H, C_6H_4, J_{H-H} = 8.8 Hz), 9.37 (SiOH). ^{29}Si NMR (solid, ppm): δ −85.42 (Q^1), −92.27 (Q^2), −102.35 (Q^3), −110.24 (Q^4). ^{13}C NMR (solid, ppm): δ 53.75 (NCH_2), 61.86 (OCH_2), 113.47 (C_6H_4), 119.08 (C_6H_4), 125.43 (C_6H_4), 131.52 (C_6H_4), 136.85 ($C_6H_4N{=}N-$), 147.81 ($C_6H_4NO_2$), 152.69 ($C_6H_4NR_2$), 155.71 ($C_6H_4N{=}N-$). FT-IR (KBr pellet, cm^{-1}): 1067−1139 (SiO). UV−vis (NMP) λ_{max}/nm 480 (ϵ = 44 700 cm^{-1} M^{-1}). Anal. Calcd for $C_{16}H_{16}N_4O_7Si_2$ (433): C, 44.44; H, 3.70; N, 12.96. Found: C, 45.21; H, 3.77; N, 12.54.

Hybrid 6b. Yield: 85%. ^{1}H NMR (DMSO, ppm) δ 3.59 (d, 4H, OCH_2, J_{H-H} = 5.5 Hz), 3.72 (d, 4H, NCH_2, J_{H-H} = 5.5 Hz), 4.18 (s, 3H, N^+CH_3), 6.4−7.3 (br, 23H, C_6H_4, BC_6H_5 and ═CH), 7.58 (d, 2H, C_6H_4, J_{H-H} = 8.7 Hz), 7.90 (d, 1H, ═CH, J_{H-H} = 15.9 Hz), 8.02 (d, 2H, C_6H_4, J_{H-H} = 8.8 Hz), 8.70 (d, 2H, C_6H_4, J_{H-H} = 8.8 Hz), 9.36 (SiOH). ^{29}Si NMR (solid, ppm): δ −84.47 (Q^1), −92.17 (Q^2), −102.25 (Q^3), −111.80 (Q^4). ^{13}C NMR (solid, ppm): δ 46.92 (CH_3), 55.62 (NCH_2), 62.85 (OCH_2), 113.58 (C_6H_4), 117.83 (C_6H_4), 121−131 (br, C_6H_4, −C═C−), 136.51 (C_6H_4), 143.66 ($C_6H_4C{=}C-$), 150.72 ($C_6H_4C{=}$ C−), 155.31 ($C_6H_4NR_2$), 166.34 ($C_5H_4NCH_3$). FT-IR (KBr pellet, cm^{-1}): 1069−1176 (Si−O). UV−vis (NMP) λ_{max}/nm 472 (ϵ = 70 200 cm^{-1} M^{-1}). Anal. Calcd for $C_{42}H_{41}BN_2O_5Si_2$ (719.8): C, 70.02; H, 5.70; N, 3.89. Found: C, 71.38; H, 6.35; N, 3.42.

Hybrid 6c. Yield: 80%. ^{1}H NMR (DMSO, ppm) δ 1.84 (m, 4H, CH_2), 3.60 (d, 4H, OCH_2, J_{H-H} = 5.8 Hz), 3.71 (d, 4H, NCH_2, J_{H-H} = 5.8 Hz), 6.81 (d, 2H, C_6H_4, J_{H-H} = 8.9 Hz), 8.09 (d, 2H, C_6H_4, J_{H-H} = 8.9 Hz), 9.38 (SiOH). ^{29}Si NMR (solid, ppm): δ −84.79 (Q^1), −93.52 (Q^2), −102.57 (Q^3), −110.65 (Q^4). ^{13}C NMR (solid, ppm): δ 30.06 (CH_2), 50.63 (NCH_2), 60.54 (OCH_2), 109.85 (C_6H_4), 126.34 (C_6H_4), 137.39 ($C_6H_4NO_2$), 153.06 ($C_6H_4NR_2$). FT-IR (KBr pellet, cm^{-1}): 1061−1119 (SiO). UV−vis (NMP): λ_{max}/nm 398 (ϵ = 18 200 cm^{-1} M^{-1}). Anal. Calcd for $C_{12}H_{16}N_2O_7Si_3$ (356): C, 40.45; H, 4.94; N, 7.87. Found: C, 41.31; H, 5.69; N, 7.52.

Hybrid 7a. Yield: 88%. ^{1}H NMR (DMSO, ppm): δ 3.62 (t, 4H, OCH_2, J_{H-H} = 5.6 Hz), 3.76 (t, 4H, NCH_2, J_{H-H} = 5.6 Hz), 6.92 (d, 2H, C_6H_4, J_{H-H} = 8.8 Hz), 7.84 (d, 2H, C_6H_4, J_{H-H} = 8.7 Hz), 7.95 (d, 2H, C_6H_4, J_{H-H} = 8.7 Hz), 8.38 (d, 2H, C_6H_4, J_{H-H} = 8.8 Hz),

9.37 (SiOH). ^{29}Si NMR (solid, ppm): δ −92.94 (Q^2), −102.83 (Q^3), −110.48 (Q^4). ^{13}C NMR (solid, ppm): δ 53.57 ($N-CH_2$), 62.40 (OCH_2), 113.75 (C_6H_4), 119.61 (C_6H_4), 125.88 (C_6H_4), 132.36 (C_6H_4), 137.12 ($C_6H_4N{=}N-$), 147.84 ($C_6H_4NO_2$), 153.27 ($C_6H_4NR_2$), 156.39 ($C_6H_4N{=}N-$). FT-IR (KBr pellet, cm^{-1}): 1066−1165 (SiO). UV−vis (NMP): λ_{max}/nm 481 (ϵ = 41 900 cm^{-1} M^{-1}). Anal. Calcd for $C_{16}H_{16}N_4O_{11}Si_4$ (552): C, 36.78; H, 3.07; N, 10.73. Found C, 37.52; H, 3.46; N, 10.89.

Hybrid 7b. Yield: 82%. ^{1}H NMR (DMSO, ppm): δ 3.58 (d, 4H, OCH_2, J_{H-H} = 5.5 Hz), 3.73 (d, 4H, NCH_2, J_{H-H} = 5.5 Hz), 4.20 (s, 3H, N^+CH_3), 6.4−7.3 (br, 23H, C_6H_4, BC_6H_5 and ═CH), 7.58 (d, 2H, C_6H_4, J_{H-H} = 8.7 Hz), 7.91 (d, 1H, ═CH, J_{H-H} = 15.8 Hz), 8.04 (d, 2H, C_6H_4, J_{H-H} = 8.8 Hz), 8.69 (d, 2H, C_6H_4, J_{H-H} = 8.7 Hz), 9.36 (SiOH). ^{29}Si NMR (solid, ppm): δ −84.97 (Q^1), −91.62 (Q^2), −101.82 (Q^3), −111.70(Q^4). ^{13}C NMR (solid, ppm): δ 46.58 (CH_3), 55.10 (NCH_2), 63.25 (OCH_2), 113.46 (C_6H_4), 118.73 (C_6H_4), 121−133 (br, C_6H_4, $-C{=}C-$), 136.94 (C_6H_4), 143.82 ($C_6H_4C{=}C-$), 150.78 ($C_6H_4C{=}C-$), 155.27 ($C_6H_4NR_2$), 164.61 ($C_5H_4N-CH_3$). FT-IR (KBr pellet, cm^{-1}): 1066−1176 (Si−O). UV−vis (NMP): λ_{max}/nm 472 (ϵ = 67 400 cm^{-1} M^{-1}). Anal. Calcd for $C_{42}H_{41}BN_2O_9Si_4$ (839.8): C, 60.00; H, 4.88; N, 3.33. Found C, 61.25; H, 5.22; N, 3.10.

Hybrid 7c. Yield: 84%. ^{1}H NMR (DMSO, ppm): δ 1.80 (m, 4H, CH_2), 3.54 (d, 4H, OCH_2, J_{H-H} = 5.8 Hz), 3.67 (d, 4H, NCH_2, J_{H-H} = 5.8 Hz), 6.76 (d, 2H, C_6H_4, J_{H-H} = 8.9 Hz), 8.07 (d, 2H, C_6H_4, J_{H-H} = 8.9 Hz), 9.37 (SiOH). ^{29}Si NMR (solid, ppm): δ −93.17 (Q^2), −101.94 (Q^3), −111.56 (Q^4). ^{13}C NMR (solid, ppm): δ 31.06 (CH_2), 51.61 (NCH_2), 60.97 (OCH_2), 110.44 (C_6H_4), 126.91 (C_6H_4), 137.35 ($C_6H_4NO_2$), 153.86 ($C_6H_4NR_2$). FT-IR (KBr pellet, cm^{-1}): 1060−1125 (SiO). UV−vis (NMP): λ_{max}/nm 398 (ϵ = 17 300 cm^{-1} M^{-1}). Anal. Calcd for $C_{12}H_{16}N_2O_{11}Si_4$ (476): C, 30.25; H, 3.36; N, 5.88. Found: C, 31.24; H, 3.87; N, 5.41.

Hybrid 8. A general procedure for the synthesis of compounds **8**−**10** is given below. To a solution of tetra(diethylamino)silane (632 mg, 2 mmol) in 25 mL of anhydrous NMP was added Disperse Red 1 (660 mg, 2 mmol) under nitrogen. The mixture was stirred at room temperature for 6 h, and then water (110 mg, 6 mmol) was added. The resulting mixture was heated to 80 °C for 24 h. The precipitate was collected by filtration. The product was washed with methanol several times and dried under vacuum at 70 °C for 24 h (640 mg, 80%). ^{29}Si NMR (solid, ppm): δ −85.74 (Q^1), −92.13 (Q^2), −101.72 (Q^3), −110.42 (Q^4). ^{13}C NMR (solid, ppm): δ 30.04 (CH_3), 51.67 (NCH_2), 54.85 (NCH_2), 54.72 (OCH_2), 61.93 (OCH_2), 112.81 (C_6H_4), 117.48 (C_6H_4), 125.47 (C_6H_4), 130.53 (C_6H_4), 142.79 ($C_6H_4N{=}N-$), 145.91 ($C_6H_4NO_2$), 151.85 ($C_6H_4NR_2$), 155.48 ($C_6H_4N{=}N-$). FT-IR (KBr, cm^{-1}): 1075−1140 (SiO). UV−vis (thin film) λ_{max}/nm 484. Anal. Calcd for $C_{16}H_{17}N_4O_5Si$ (373): C, 51.47; H, 4.56; N, 15.01. Found: C, 52.03; H, 4.92; N, 14.68.

Hybrid 9. Yield: 90%. ^{29}Si NMR (solid, ppm): δ −92.27 (Q^2), −101.85 (Q^3), −109.81 (Q^4). ^{13}C NMR (solid, ppm): δ 31.04 (CH_3), 51.26 (NCH_2), 52.65 (NCH_2), 54.68 (OCH_2), 62.27 (OCH_2), 112.65 (C_6H_4), 117.59 (C_6H_4), 126.72 (C_6H_4), 131.03 (C_6H_4), 143.34 ($C_6H_4N{=}N-$), 146.21 ($C_6H_4NO_2$), 152.75 ($C_6H_4NR_2$), 156.18 ($C_6H_4-N{=}N-$). FT-IR (KBr, cm^{-1}): 1070−1144 (SiO). UV−vis (thin film): λ_{max}/nm 484. Anal. Calcd for $C_{16}H_{17}N_4O_{3.5}Si_2$ (425): C, 45.17; H, 4.00; N, 13.18. Found: C, 45.87; H, 4.45; N, 12.74.

Hybrid 10. Yield: 86%. ^{29}Si NMR (solid, ppm): δ −92.51 (Q^2), −103.08 (Q^3), −111.48 (Q^4). ^{13}C NMR (solid, ppm): δ 31.24 (CH_3), 52.17 (NCH_2), 52.72 (NCH_2), 55.46 (OCH_2), 62.51 (OCH_2), 113.29 (C_6H_4), 118.73 (C_6H_4), 125.65 (C_6H_4), 131.22 (C_6H_4), 143.58 ($C_6H_4N{=}N-$), 146.71 ($C_6H_4NO_2$), 152.36 ($C_6H_4NR_2$), 156.60 ($C_6H_4N{=}N-$). FT-IR (KBr, cm^{-1}): 1068−1146 (Si−O). UV−vis (thin film): λ_{max}/nm 483. Anal. Calcd for $C_{16}H_{17}N_4O_{5.5}Si_3$ (485): C, 39.59; H, 3.51; N, 11.54. Found: C, 40.17; H, 3.89; N, 11.40.

Polymeric Thin Films. For **5**−**7**, a solution of the hybrid was prepared by dissolving it into NMP, filtering through 0.2-μm syringe filters, and then spin-coating it onto a glass substrate with an indium−tin oxide (ITO) conductive layer. The film was dried under vacuum at 60 °C for 24 h. It was heated to 100−220 °C over 40 min with the application of dc electric fields from 3.5 to 4.5 KV using a corona discharge setup (1.0 cm of a tip-to-plane gap) and then cooled to room temperature over a period of 30 min. For insoluble hybrids **8**−**10**, the film was spin-coated before condensation, dried under vacuum for 2 days, and then cured at 120−140 °C for 2 h in the presence of an electric field (4.2 KV) to form chromophore-aligned siloxane networks.

Acknowledgment. This work was supported by the NSERC of Canada and FCAR (Quebec, Canada). We would also like to thank Dr. Jianyao Wu and Grant Kiehne (Northwestern University, Evanston, Illinois) for their help in carrying out the second harmonic generation experiments.

JA983274J